Liquid-drop model for the size-dependent melting of low-dimensional systems

K. K. Nanda,* S. N. Sahu,† and S. N. Behera‡
Institute of Physics, Sachivalaya Marg, Bhubaneswar 751005, India
(Received 20 August 2001; published 29 July 2002)

Empirical relations are established between the cohesive energy, surface tension, and melting temperature of different bulk solids. An expression for the size-dependent melting for low-dimensional systems is derived on the basis of an analogy with the liquid-drop model and these empirical relations, and compared with other theoretical models as well as the available experimental data in the literature. The model is then extended to understand (i) the effect of substrate temperature on the size of the deposited cluster and (ii) the superheating of nanoparticles embedded in a matrix. It is argued that *the exponential increase in particle size with the increase in deposition temperature can be understood* by using the expression for the size-dependent melting of nanoparticles. Superheating is possible when nanoparticles with a lower surface energy are embedded in a matrix with a material of higher surface energy in which case the melting temperature depends on the amount of epitaxy between the nanoparticles and the embedding matrix. The predictions of the model show good agreement with the experimental results. A scaling for the size-dependent melting point suppression is also proposed.

DOI: 10.1103/PhysRevA.66.013208 PACS number(s): 36.40.Ei, 21.10.Dr, 05.70.Np

I. INTRODUCTION

It is well established both experimentally and theoretically that the melting temperature (T_m) of nanoparticles depends on the particle size [1–30]. For substrate-supported nanoparticles with relatively free surface, the melting temperature decreases with decreasing particle size [1–12]. In contrast, as per the existing experimental evidence for embedded nanoparticles, the melting temperature can be lower than the bulk melting point for some matrices while the same nanoparticles embedded in some other matrices can exhibit superheating to temperatures higher than the bulk melting point [20–30]. Experimental results of Sheng *et al.* [24,25] reveal that the enhancement or depression of the melting temperature of the embedded nanoparticles depends on the epitaxy between the nanoparticles and the embedding matrix. While the size-dependent depression of melting point has been theoretically modeled by several authors [3–5,14–19], a proper understanding of the superheating of embedded nanoparticles is lacking. Based on the size-dependence of the amplitudes of the atomic vibrations and the Lindemann's criterion, Jiang *et al.* [28,29] have developed a model for the superheating of nanoparticles embedded in a matrix, according to which the superheating is possible if the diameter of the constituent atoms of the matrix is smaller than the atomic diameter in the nanoparticles.

In this paper, empirical relations between cohesive energy, surface tension, and melting temperature of different bulk solids are established. On the basis of an analogy with the liquid-drop model and making use of these empirical relations, an expression for the size-dependent melting for low-dimensional systems is derived and compared with other theoretical models, and experimental data available in the literature. The expression so derived is then extended to understand other phenomena, such as (i) how substrate temperature effects the growth of the size of the deposited nanoparticles and (ii) the superheating of nanoparticles embedded in a matrix. It is argued that depending upon the epitaxy between the nanoparticles and the embedding matrix, superheating is possible if the surface energy of the nanomaterial is smaller than that of the embedding matrix. A scaling for the size-dependent melting point suppression is also proposed.

II. EMPIRICAL RELATION FOR SIZE-DEPENDENT MELTING

A. Cohesive energy

One of the many successes of the liquid-drop model lies in providing an intuitive explanation of the phenomenon of spontaneous fission of some nuclei. Atomic clusters and nanoparticles being finite systems, their properties are dominated by the surface atoms, therefore their binding energy can be effectively represented by the volume and surface dependent terms as in the liquid-drop model. From this point of view the melting of atomic clusters and nanoparticles can be understood by scaling the cohesive energy to the melting temperature. According to the liquid-drop model [31,32], the total cohesive energy (E_b) of a nanoparticle of N atoms is equal to the volume energy $a_v N$ minus the surface energy $4\pi r_a^2 N^{2/3}\gamma$, the latter term arising from the presence of atoms on the surface. Hence, the cohesive energy per atom, i.e., $E_b/N = a_{v,d}$ is given by

$$a_{v,d} = a_v - \frac{4\pi r_a^2 \gamma}{N^{1/3}} = a_v - a_s N^{-1/3}, \tag{1}$$

where a_v represents the cohesive energy of bulk, r_a is the radius of one atom deduced from the atomic volume ($\nu_0 = 4\pi r_a^3/3$), and γ is the coefficient of surface energy of the material. This expression is the same as the binding energy

*Present address: Gerhard-Mercator University Duisburg, Process- and Aerosol Measurement Technology, 47048 Duisburg, Germany. Email address: nanda@uni-duisburg.de
†Email address: sahu@iopb.res.in
‡Email address: snb@iopb.res.in

per nucleon obtained from the liquid-drop model which is known to be so successful in explaining the mass of the atomic nuclei [33]. The model has also been successfully applied recently to explain the size-dependent lattice contraction associated with reduced dimensions [34]. The number of atoms in a spherical nanoparticle of diameter "d" being

$$N=\frac{d^3}{(2r_a)^3},$$

the expression for the cohesive energy per atom becomes

$$a_{v,d}=a_v-\frac{6\nu_0\gamma}{d}. \tag{2}$$

Equation (2) implies that the cohesive energy per atom decreases as the particle size decreases and the rate of decrease depends on the values of the atomic volume (ν_0) and the coefficient of surface energy (γ). This provides a qualitative understanding of the size dependence of the amount of energy required to remove an atom from a cluster [35].

B. Empirical relation between cohesive energy and melting temperature

It has been shown by Rose *et al.* [36] that there exists a universal relation between the cohesive energy and surface energy, i.e.,

$$a_s=0.82a_v,$$

which has been experimentally [31] verified for clusters of Li, Na, and K. Tateno [37] has derived an expression for the melting temperature (T_m) of the bulk material in terms of the cohesive energy, based on the Lindemann's criterion of melting, which is

$$T_m=na_vf^2/3k_BZ, \tag{3}$$

where n is the exponent of the repulsive part of the interaction potential between constituent atoms, Z is the valency of the atoms, f is the characteristic fraction which is the ratio of the atomic displacement at T_m to the interatomic separation at equilibrium, and k_B is the Boltzmann constant. As Eq. (3) indicates a relation between the bulk cohesive energy and the melting temperature, the variation of the melting temperature of nanoparticles with particle size will immediately follow if one uses $a_{v,d}$ from Eq. (2) in place of a_v in Eq. (3) [38]. However, the cohesive energy per atom, if derived from the liquid-drop model, should relate to the liquid-gas transition. Therefore, it is our belief that the melting temperature can be related to the cohesive energy per coordination number. Therefore, to obtain an empirical relation for the size-dependence of melting temperature of nanoparticles, we plot the cohesive energy per coordination of different elemental solids against the melting temperature as shown in Fig. 1. The data for cohesive energy per atom are taken from Refs. [39,40] and the cohesive energy per coordination number is determined from the cohesive energy per atom by using the following formula [41]:

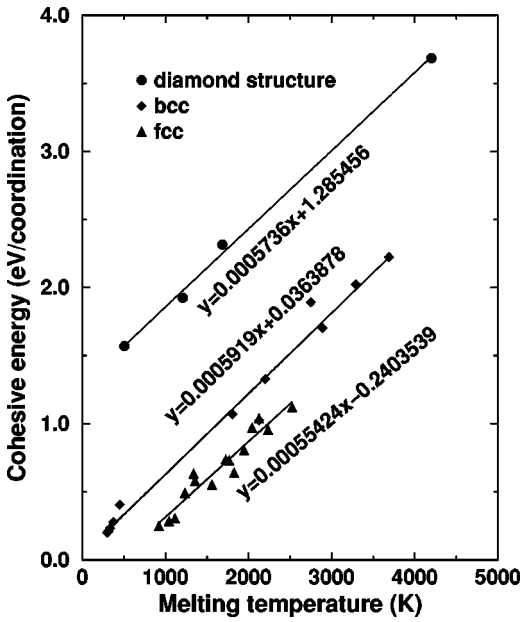

FIG. 1. Plot of cohesive energy per coordination vs melting temperature of different elements. The data for cohesive energy per atom are taken from Refs. [39,40], whereas the cohesive energy per coordination is estimated from the cohesive energy per atom by using Eq. (4).

$$(\text{Cohesive energy per coordination})=\frac{(\text{Cohesive energy per atom})}{(\text{Coordination number per atom})}, \tag{4}$$

where coordination number per atom is the coordination number divided by two as each coordination number is shared by two atoms. Interestingly, a linear relationship is found for different structures with almost the same slopes. Assuming the value of the slope for C, Si, Ge, and Sn as obtained from Fig. 1 to provide a reasonable representation for all solids, one can express the cohesive energy per coordination (a_v) in term of the melting temperature ($T_{\rm mb}$) of the bulk material as

$$a_v=0.000\,573\,6\,T_{\rm mb}+c, \tag{5}$$

where c is the intercept of the straight line.

C. Empirical relation between surface tension and melting temperature

The surface energy and the melting temperature of different elemental solids are plotted against the atomic number in Fig. 2(a). The data are taken from Ref. [42]. Figure 2(a) predicts a definite correlation between the surface tension and the bulk melting temperature which further motivated us to plot the surface energy as a function of the bulk melting temperature which is shown in Fig. 2(b). It can be noted from Fig. 2(b) that the data can be fitted into a straight line which yields a slope $0.915\,665\,5$ mJ/m^2 K and an intercept 133.2806 mJ/m^2. This clearly indicates that the higher the surface energy, the higher is the bulk melting temperature.

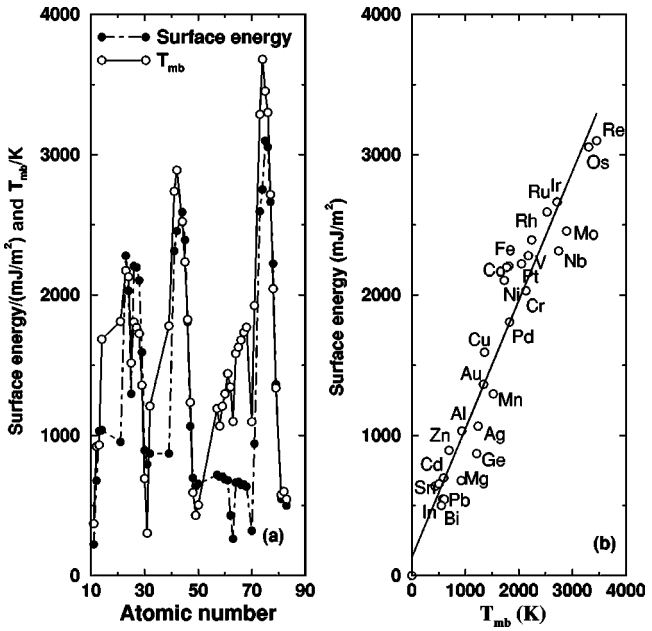

FIG. 2. (a) The surface energy and the melting temperature are plotted against the atomic number; (b) the surface energy is plotted against the bulk melting temperature yielding a straight line. The data are taken from Ref. [42].

D. Size-dependent melting of nanoparticles

As argued in Sec. II B there exists a universal relation between cohesive energy and surface energy which we assume to hold for the nanoparticles as well and express the cohesive energy in terms of the melting temperature (T_m) of the nanoparticles as

$$a_{v,d} = 0.000\,573\,6\,T_m + c.$$

Based on this relation and Eqs. (2) and (5), T_m can be expressed in terms of the bulk melting temperature (T_{mb}) as

$$T_m = T_{\mathrm{mb}} - \frac{6\nu_0\gamma}{0.000\,573\,6\,d} \Rightarrow \frac{T_m}{T_{\mathrm{mb}}} = 1 - \frac{6\nu_0}{0.000\,573\,6\,d}\left(\frac{\gamma}{T_{\mathrm{mb}}}\right) = 1 - \frac{\beta}{d}. \tag{6}$$

Similar expressions for size dependent melting for spherical nanoparticles has also been derived from thermodynamic arguments [2,3] and from a model based on surface-phonon instability [15]. Using the known values of υ_0, γ, and T_{mb}, the value of β for different elements is estimated and presented in Table I. It may be noted that the value of β obtained from the empirical relation is consistent with that of the phonon-instability model. In order to test this empirical formulation further, the results for the liquid-drop model are compared with the experimental data [1,12] of Pb and In. Shown in Figs. 3(a) and 3(b) are the plots of the normalized melting temperature (T_m/T_{mb}) versus inverse of the particle diameter (d). The solid lines are the theoretical prediction according to Eq. (6), whereas the dot-dashed line in Fig. 3(b) is the prediction of the Landau theory as developed by Sakai [17] for Pb. It can be noted from Fig. 3 that the agreement with experiment for In is excellent. On the other hand, there is a disagreement between experiment and the theoretical predictions for Pb particles, especially in the intermediate size range, whereas there is agreement for particles with lower and higher sizes. However, in the intermediate size range the data can be accounted for (dashed line) if the value of β is chosen as half the value given in Table I. A possible explanation for this is provided in a later section. Further, it can be noted that the prediction of the liquid-drop model is in good agreement with that (dot-dashed line) of Sakai [17].

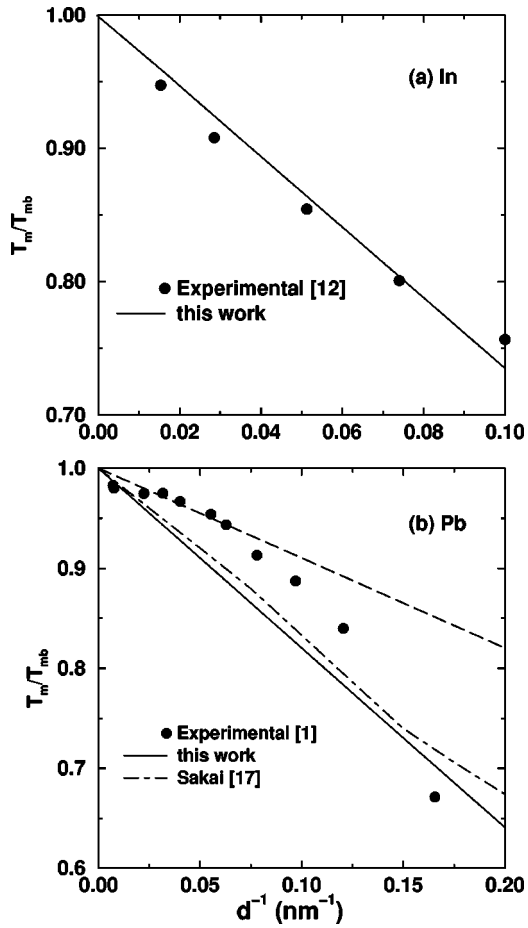

FIG. 3. Comparison of experimental size-dependent melting temperature depression of In (a) and Pb (b) nanoparticles with different models. The data are taken from Refs. [12] and [1] for In and Pb, respectively.

E. Melting of pancake-shaped nanoparticles

For particles of spherical geometry with diameter d, the surface to volume ratio $A = 6/d$, which when substituted in Eq. (6) gives

$$\frac{T_m}{T_{\mathrm{mb}}} = 1 - \frac{\beta}{6}A.$$

On the other hand, for a particle with cylindrical geometry of height l and diameter d, the surface to volume ratio (A) is

TABLE I. Comparison of our model with the surface phonon-instability model.

Elements	γ (mJ/m^2) Ref. [28]	T_{mb} (K)	γ/T_{mb} (mJ/m K)	Atomic volume per mole (cm^3)	β (nm)	β (nm) Ref. [14]
Na	223	371	0.601	23.78	1.487	0.73, 2.05
Mg	679	922	0.7364	14.0	1.1211	0.9, 1.54
Al	1032	933.25	1.106	10.0	1.2	1.14
Si	1038	1685	0.616	12.06	0.8454	1.88
Sc	954	1812	0.5265	15.00	0.8573	1.04
V	2280	2175	1.0483	8.32	0.944	1.05, 1.36
Cr	2031	2130	0.953	7.23	0.744	1.05
Mn	1297	1517	0.855	7.35	0.672	
Fe	2206	1809	1.219 46	7.09	0.942 32	1.09
Co	2197	1768	1.242 65	6.67	0.9	1.0
Ni	2104	1726	1.219	6.59	0.87	1.10
Cu	1592	1357.6	1.172 66	7.11	0.9	1.02
Zn	895	692.73	1.292	9.16	1.284	1.06
Ga	794	302.9	2.6213	11.80	3.36	1.07, 2.78
Ge	870	1210.4	0.719	13.63	1.06	2.3, 3.33
Y	871	1782	0.4888	19.88	1.055	1.42
Nb	2314	2740	0.8445	10.83	0.9921	1.43
Mo	2546	2890	0.881	9.38	0.9	0.99, 1.58
Ru	2591	2523	1.027	8.17	0.91	1.01
Rh	2392	2236	1.07	8.28	1.0377	1.13
Pd	1808	1825	0.9907	8.56	0.9517	0.88, 1.43
Ag	1065	1234	0.863	10.27	0.965 64	1.27
Cd	697	594.18	1.173	13.0	1.655	1.07
In	638	429.76	1.484 55	15.76	2.65	1.95
Sn	654	505.06	1.295	16.29	2.2784	1.57
La	718	1193	0.601 84	22.39	1.463	1.64
Ce	706	1068	0.661	20.69	1.484 54	1.17
Pr	707	1208	0.5853	20.80	1.3215	2.03
Nd	687	1297	0.53	20.59	1.1846	1.54
Pm	680	1441	0.472	20.23	1.0365	
Sm	431	1345	0.32	19.98	0.694	0.86
Eu	264	1099	0.24	28.97	0.755	0.95
Gd	664	1585	0.42	19.90	0.9073	1.36
Tb	669	1629	0.4107	19.3	0.86	1.41
Dy	648	1680	0.3857	19.01	0.796	0.98
Ho	650	1734	0.275	18.74	0.763	0.91
Er	630	1770	0.356	18.46	0.7134	0.97
Yb	320	1097	0.2917	24.84	0.7865	1.09
Lu	940	1925	0.4883	17.78	0.942 43	1.23
Ta	2595	3287	0.7895	10.85	0.94	1.2
W	2753	3680	0.7481	9.47	0.772	1.1
Re	3100	3453	0.8978	8.86	0.8635	0.99
Os	3055	3300	0.925 76	8.42	0.8453	1.07
Ir	2664	2716	0.981	8.52	0.908	1.08
Pt	2223	2045	1.087	9.09	1.07	0.89
Au	1363	1337.6	1.019	10.21	1.1281	0.92
Tl	547	577	0.948	17.22	1.7763	1.11
Pb	544	600.6	0.9058	18.26	1.7957	0.98
Bi	501	544.52	0.92	21.31	2.1273	0.86

$$A = 4/d + 2/l$$

and hence, the melting temperature can be written as

$$\frac{T_m}{T_{\rm mb}} = 1 - \frac{\beta}{6}\left(\frac{4}{d} + \frac{2}{l}\right). \tag{7}$$

For a pancakelike geometry of the nanoparticles, the height l is much less than d and $A \gg 6/d$. Therefore, the melting temperature of these particles would be lower as compared to a spherical particle of diameter d.

F. Melting of thin wires ($l \gg d$)

For a thin wire of length l and diameter d, $l \gg d$ and hence, the melting temperature is given by

$$\frac{T_m}{T_{\rm mb}} = 1 - \frac{2\beta}{3d}. \tag{8}$$

This relation has some similarity to the size dependence of melting of thin wires as described by Gülseren *et al.* [19]. The only difference is that in the present case the melting temperature of a thin wire is suppressed by a factor which is two third of the suppression for a spherical nanoparticle, whereas a molecular dynamics (MD) simulation [19] predicts the melting temperature to be suppressed by approximately half the amount of a spherical particle.

G. Melting of thin films ($l \ll d$)

In case of a thin film, on the other hand, $l \ll d$ and the melting temperature is given by

$$\frac{T_m}{T_{\rm mb}} \cong 1 - \frac{\beta}{3l}. \tag{9}$$

This implies that the suppression of the melting temperature of a thin film depends mainly on the thickness of the film, which is in agreement with reported results [18].

H. General expression of T_m for low-dimensional systems

Comparing Eqs. (6), (8), and (9) for a given size of the particle, the diameter of the wire, and the thickness of the film, one gets

$$\left.\frac{T_{\rm mb} - T_m}{T_{\rm mb}}\right|_{\rm sphere} : \left.\frac{T_{\rm mb} - T_m}{T_{\rm mb}}\right|_{\rm wire} : \left.\frac{T_{\rm mb} - T_m}{T_{\rm mb}}\right|_{\rm film} = 3:2:1, \tag{10}$$

which implies that the rate of decrease of the melting temperature for different low-dimensional systems is in the ratio (sphere:wire:film)=(3:2:1), a result in accordance with the predicted behavior from thermodynamical considerations [16]. Based on Eq. (10) the expression for size-dependent melting, in general, can be written as

$$\frac{T_m}{T_{\rm mb}} = 1 - \frac{\beta}{zd}, \tag{11}$$

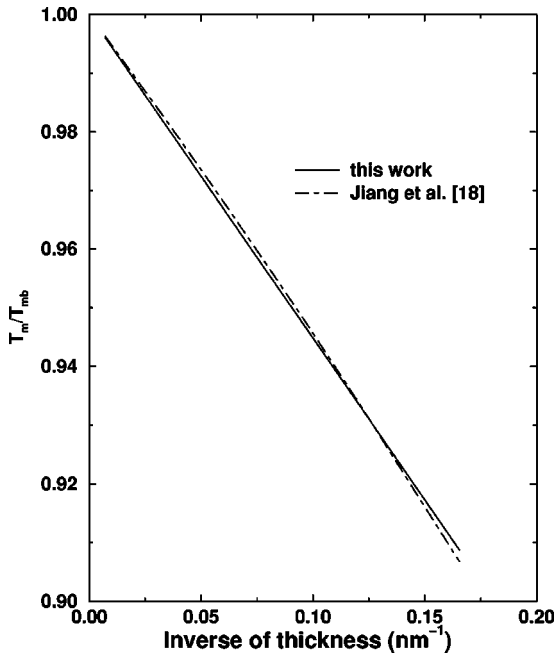

FIG. 4. Comparison of our model with the model of Shi and co-workers [18] for Pb thin film.

with $z=1$, 3/2, and 3 for nanoparticles, nanowires, and thin films, respectively. It may be noted that in Eq. (11), d represents the diameter in case of nanoparticles and nanowires, whereas it represents the thickness in case of thin films. The predictions of the liquid-drop model can now be compared with the theoretical predictions of Jiang *et al.* [18], the latter based on the size-dependent atomic vibrations and Lindemann's criterion. The comparison of the predictions of these two models for Pb thin films ($z=3$) is shown in Fig. 4. The values of β are taken from Table I. As can be seen from the figure, both the models are found to be consistent for Pb thin films.

I. Superheating of nanoparticles

In the case of embedded nanoparticles if their surface atoms are completely saturated with the atoms of the surrounding matrix, then the coefficient of surface energy (γ) will be effectively altered at the interface, resulting in the modification of Eq. (2) as

$$a_{v,d} = a_v - \frac{6\nu_0(\gamma - \alpha\gamma_M)}{d}, \tag{12}$$

where γ_M is the coefficient of surface energy of the surrounding material and α represents the amount of correlation between the atoms of the nanoparticles and those of the surrounding matrix; $\alpha=0$ for free nanoparticles and $\alpha=1$ if there is epitaxy between nanocrystals and the surrounding matrix. In the case of epitaxy $\alpha=1$, the size dependent melting, as given by the ratio of the melting temperatures of the nanoparticles to that of their corresponding bulk, can be expressed following Eqs. (6) and (12) as

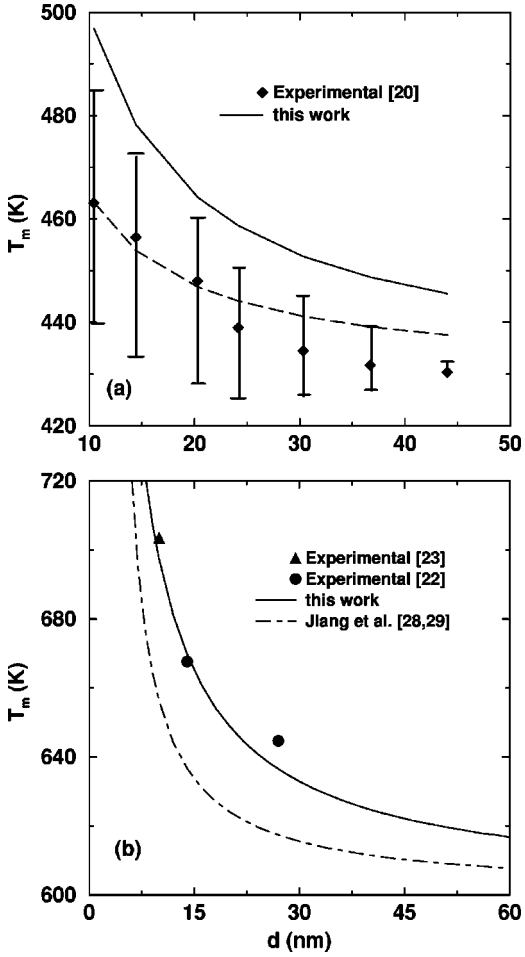

FIG. 5. Comparison of experimental size-dependent superheating of In (a) and Pb (b) nanoparticles embedded in Al matrix with different models. The data are taken from Ref. [20] and Refs. [22], [23] for In and Pb, respectively. The surface energy (γ) of In, Pb, and Al is taken from Table I.

$$\frac{T_m}{T_{\mathrm{mb}}} \cong 1 - \frac{\beta}{d}\left(1 - \frac{\gamma_M}{\gamma}\right). \tag{13}$$

It can be noted from Eq. (13) that the nanoparticles will melt above the bulk melting temperature if $\gamma_M > \gamma$. In order to test the validity of this formulation, the results of the liquid-drop model are compared in Figs. 5(a) and 5(b) with the experimental data for the size-dependent superheating of In and Pb nanoparticles embedded in Al matrix [20,22,23] and in doing so the coefficient of the surface energy of In, Pb, and Al are taken from Table I. The results from the model of Jiang *et al.* [28,29] are also plotted for comparison. It may be noted that the liquid-drop model is in excellent agreement with the experimental data of Pb particles in Al matrix but overestimates the melting temperature for In particles in Al matrix. However, the data for In particles embedded in Al matrix can be accounted (dashed line) for by taking the value of β to be half of that given in Table I. In contrast, the model developed by Jiang *et al.* underestimates the size-dependent superheating of Pb nanoparticles embedded in Al matrix as shown in Fig. 5(b), even though both the liquid-drop model and the model of Jiang *et al.* are consistent for thin films (see Fig. 4). Recently, Zhang *et al.* [30] have observed the superheating by 6 °C for the 20 nm thick Pb films sandwiched within Al layers while for the same system the liquid-drop model predicts a superheating by 16 °C. The discrepancy between the predictions of the present theory and the experimental data of (i) In particles embedded in Al matrix and (ii) Pb films sandwiched between Al layers can be attributed to the epitaxy between In and Al. Recalling from Fig. 3(b) that the size-dependent melting temperatures of Pb nanoparticles in the intermediate size range can be understood by taking the value of β to be half of the value given in Table I, it is not surprising because the shape of the Pb nanoparticles resembles a disk [1] and are supported by a substrate implying that only half of the surface is free.

J. Melting of atomic clusters

An irregular variation of melting temperature of Ar clusters with size was predicted from theoretical calculations [43]. For rare-gas atoms the completion of geometrical shell occurs at cluster sizes of $N = 13$, 55, 147, 309,... and the corresponding local maxima of melting temperatures were found for these magic numbers which can be attributed to the increase in binding energy per atom at shell closure. Recently, similar irregular variation of melting temperature was observed experimentally [44] for Na clusters for which the peaks in the abundance distributions occur at cluster sizes of $N = 59$, 93, 139, 197,..., whereas the local maxima of melting occurs for $N = 93$, 142,... . For alkali-atom clusters the stability, and hence the abundance, is determined by electronic shell closure which is predicted to occur at $N = 58$, 92, 138, 198 ± 2, 258 ± 3, etc. However, since the measurements are done on free clusters, in the ionic state, clusters with one more atom will correspond to the electronic shell closure, which is consistent with the measurement. However, since the present liquid-drop model does not take into account the shell closure effects on the binding energy, a discussion of the melting of small atomic clusters is beyond the scope of the model.

K. Effect of deposition temperature on particle size

The present understanding of the phenomenon of the size-dependent melting can provide an explanation of the dependence of the growth of deposited nanoparticles on deposition temperature or the substrate temperature. For a given deposition or substrate temperature, there will be a critical size of the particle in the cluster beam, such that, any particle larger than this will be deposited as such. On the other hand if the incident cluster size is smaller than the critical size, the particle will melt upon deposition and they will coagulate to produce larger clusters. Once a larger cluster is formed, it solidifies and stops further coagulation. This implies that the deposition temperature should be as low as possible to obtain smaller size particles. Based on the above discussion, it can be shown from Eq. (6) that the stable clusters with size d_s depends on the substrate temperature T_s as

$$\frac{T_s}{T_{\rm mb}} = 1 - \frac{\beta}{d_s} \Rightarrow d_s = \frac{\beta}{(1 - T_s/T_{\rm mb})} \cong \beta \exp\left(\frac{T_s}{T_{\rm mb}}\right). \quad (14)$$

This implies that the cluster size and hence the number of atoms in the deposited nanoparticle increases with increasing substrate temperature, which is in good agreement with the experimental observation [45]. It can be inferred from Eq. (14) that d_s can be estimated if β and T_s are known. This result of the liquid-drop model can now be compared with the experimental data on the substrate-temperature-dependent particle size. Mitch *et al.* [46] have found that the crystallinity of a 0.8 nm thick Bi film disappears at 110 K. Similarly, the crystallinity of a Pb wire of diameter 3.0 nm in a carbon nanotube disappears [47] at room temperature. Taking $T_s = 110$ K, $\gamma = 501$ mJ/m^2, $T_{\rm mb} = 544.5$ K, $\nu_0 = 0.107172$ nm^3, and $z = 3$ for a Bi film, it is estimated that $d_s = 0.9$ nm. Similarly, taking $T_s = 300$ K, $\gamma = 544$ mJ/m^2, $T_{\rm mb} = 600.6$ K, $\nu_0 = 0.121\,287$ nm^3, and $z = 3/2$ for a Pb wire, it is estimated that $d_s = 2.4$ nm, and taking $T_s = 300$ K, $\gamma = 654$ mJ/m^2, $T_{\rm mb} = 505.1$ K, $\nu_0 = 0.107\,637$ nm^3, and $z = 1$ for Sn particles, it is estimated that $d_s = 5.6$ nm. In this context it is worth pointing out that Oshima *et al.* [10] observed a pseudocrystalline phase between that of a solid and a liquid for $d < 5.0$ nm in the case of Sn nanoparticles which is very close to the size predicted from the present model. The thickness of the Bi thin film, the diameter of the Pb wire, and the diameter of the Sn particle are found to agree well with the experimental results which provide support to the validity of the present model.

III. SCALING LAW FOR SIZE-DEPENDENT MELTING

With the quantitative understanding of the effect of substrate temperature on particle size, it is believed that a scaling for the size-dependent melting point suppression for different materials is possible. It can be noted from Eq. (6) that the size-dependent melting curves for all the materials will collapse into a single curve if the data are plotted as $T_m/T_{\rm mb}$ versus β/d where $T_{\rm mb}$ and β are material specific. In order to demonstrate the scaling of size-dependent melting, the data [11] for Pb, Sn, In, and Bi nanoparticles are plotted as $T_m/T_{\rm mb}$ versus $1/d$ in Fig. 6(a) and the same data are plotted as $T_m/T_{\rm mb}$ versus β/d in Fig. 6(b). The solid line in Fig. 6(b) represents the results from the liquid-drop model. Interestingly, the size-dependent melting curves are found to obey scaling behavior except for Bi. It is also noted that the experimental melting temperatures are somewhat higher than that predicted by the liquid-drop model. It is believed that the discrepancy can be attributed to the interaction between these nanoparticles and the carbon substrate on which these are deposited and the interaction of Bi particles is probably weaker as compared to other nanoparticles.

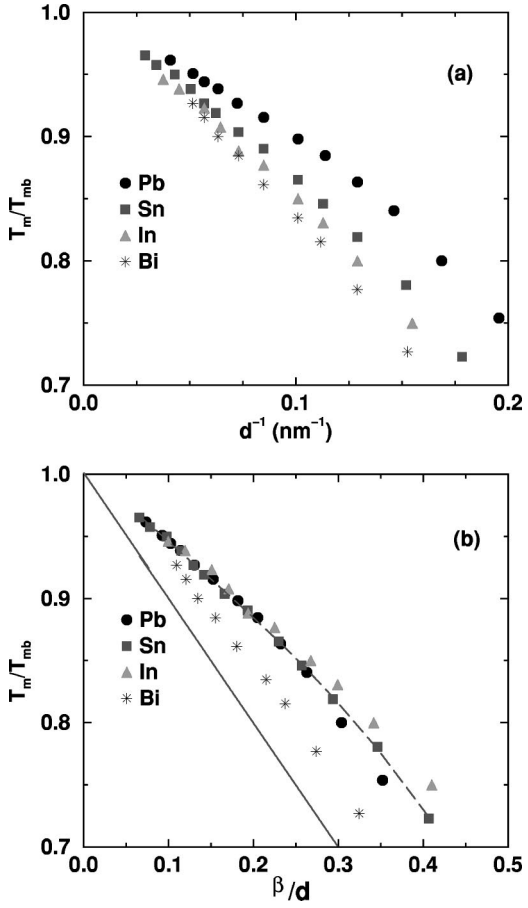

FIG. 6. (a) The size-dependent melting of Pb, Sn, In, and Bi nanoparticles plotted as $T_m/T_{\rm mb}$ vs $1/d$. (b) The size-dependent melting plotted as $T_m/T_{\rm mb}$ vs β/d. The data are taken from Ref. [11] and the values of β are taken from Table I. The solid line is the theoretical curve based on the liquid-drop model and the dashed line is guide to the eye.

IV. DISCUSSION

It is well established that the change in the melting temperature of nanoparticles with their size is a surface initiated process [9,17]. The MD simulation also corroborates to this and shows that the melting of a thin wire starts from the curved surface rather than the flat surface [19]. At the surface, the number of nearest neighbors of a given atom is smaller than that in the bulk. Therefore, the surface starts to disorder on raising the temperature even though the bulk retains its ordered state. This is the mechanism of surface-induced melting. The relative availability of surface atoms can be increased by reducing the particle size, thereby lowering the surface-induced melting temperature of the particle. In this paper it is shown that this is in accordance with the simple minded liquid-drop-like model which predicts the decrease of the melting temperature to be proportional to the surface-to-volume ratio. This model not only explains the size-dependent melting temperature depression of free nanoparticles, but also explains quantitatively the size-dependent superheating of nanoparticles embedded in a matrix. This simple phenomenological liquid-drop model also successfully predicts the critical size below which the crystallinity of a material disappears at a given deposition or substrate temperature. The estimated size is found to be in excellent agreement with the experimental observations.

Some of the technical advantages of the low melting temperatures of small nanoparticles are: (1) the ability to fuse

nanoparticles to form a film at a relatively modest temperature indicating that nanoparticles may provide a new low-temperature route to thin-film growth, (2) possibility of soldering at relatively low temperatures using nanoparticles, (3) possibility of controlling the growth process of nanoparticles by controlling the deposition or substrate temperature. It is also shown that the superheating of nanoparticles embedded in a matrix strictly depends on the epitaxy at the interface. This allows for the possibility of elevating the temperature at which the instability against melting of the low-dimensional materials sets in.

V. CONCLUSION

It is shown that the simple minded liquid-drop model can explain the size-dependent melting associated with the size and geometry of the low-dimensional systems. The size-dependent superheating of nanoparticles embedded in a matrix is also understood using this model which predicts that the superheating is possible if the coefficient of surface energy of the matrix is higher than that of the nanomaterials. The existence of a scaling law for the size-dependent melting point suppression is demonstrated.

ACKNOWLEDGMENTS

One of the authors (K.K.N.) acknowledges helpful correspondence with Professor W. A. Harrison on the relation between cohesive energy per coordination and cohesive energy per atom. The work was supported by the Indo-French Centre (IFCPAR) through Project No. IFCPAR 1508-4.

[1] C. J. Coombes, J. Phys. F: Met. Phys. **2**, 441 (1972).
[2] Ph. Buffat and J.-P. Borel, Phys. Rev. A **13**, 2287 (1976).
[3] P. R. Couchman and W. A. Jesser, Nature (London) **269**, 481 (1977).
[4] T. Castro, R. Reifenberger, E. Choi, and R. P. Andres, Phys. Rev. B **42**, 8548 (1990).
[5] A. N. Goldstein, C. M. Echer, and A. P. Alivisatos, Science **256**, 1425 (1992).
[6] A. N. Goldstein, Appl. Phys. A: Mater. Sci. Process. **A62**, 33 (1996).
[7] R. Kofman *et al.*, Z. Phys. D: At., Mol. Clusters **20**, 267 (1991); R. Garrigos, P. Cheyssac, and R. Kofman, *ibid.* **12**, 497 (1989).
[8] T. Ben David *et al.*, Philos. Mag. A **71**, 1135 (1995).
[9] G. L. Allen, R. A. Bayles, W. W. Gile, and W. A. Jesser, Thin Solid Films **144**, 297 (1986).
[10] Y. Oshima and K. Takayanagi, Z. Phys. D: At., Mol. Clusters **27**, 287 (1993).
[11] V. P. Skripov, V. P. Koverda, and V. N. Skokov, Phys. Status Solidi A **66**, 109 (1981).
[12] J. F. Fócza, A. Barna, and P. B. Barna, J. Vac. Sci. Technol. **6**, 472 (1969).
[13] T. P. Martin, Phys. Rep. **273**, 199 (1996).
[14] K. J. Hanszen, Z. Phys. **157**, 523 (1960).
[15] M. Wautelet, J. Phys. D **24**, 343 (1991).
[16] M. Wautelet, Phys. Lett. A **246**, 341 (1998).
[17] H. Sakai, Surf. Sci. **351**, 285 (1996); **348**, 387 (1996).
[18] Q. Jiang *et al.*, Thin Solid Films **312**, 357 (1998).
[19] O. Gülseren, F. Ercolessi, and E. Tosatti, Phys. Rev. B **51**, 7377 (1995).
[20] H. Saka, Y. Nishikawa, and T. Imura, Philos. Mag. A **57**, 895 (1988).
[21] H. W. Sheng, K. Lu, and E. Ma, Nanostruct. Mater. **10**, 865 (1998).
[22] L. Grabaek *et al.*, Phys. Rev. Lett. **64**, 934 (1990).
[23] K. Chattopadhyay and R. Goswami, Prog. Mater. Sci. **42**, 287 (1997).
[24] H. W. Sheng, G. Ren, L. M. Peng, Z. Q. Hu, and K. Lu, Philos. Mag. Lett. **73**, 179 (1996).
[25] H. W. Sheng, G. Ren, L. M. Peng, Z. Q. Hu, and K. Lu, J. Mater. Res. **12**, 119 (1997).
[26] T. Ohashi, K. Kuroda, and H. Saka, Philos. Mag. B **65**, 1041 (1992).
[27] F. G. Shi, J. Mater. Res. **9**, 1307 (1994).
[28] Q. Jiang, Z. Zhang, and J. C. Li, Chem. Phys. Lett. **322**, 549 (2000).
[29] Z. Zhang, Z. C. Li, and Q. Jiang, J. Phys. D **33**, 2653 (2000).
[30] L. Zhang, Z. H. Jin, L. H. Zhang, M. L. Sui, and K. Lu, Phys. Rev. Lett. **85**, 1484 (2000).
[31] C. Bréchignac *et al.*, J. Chem. Phys. **101**, 6992 (1994).
[32] U. Näher *et al.*, Phys. Rep. **285**, 245 (1997).
[33] R. R. Roy and B. P. Nigam, *Nuclear Physics Theory and Experiment* (Wiley, New York, 1967), Chap. 5.
[34] K. K. Nanda, S. N. Behera, and S. N. Sahu, J. Phys.: Condens. Matter **13**, 2861 (2001).
[35] J. Borggreen *et al.*, Phys. Rev. A **62**, 013 202 (2000); F. Chandezon *et al.*, Phys. Rev. B **55**, 5485 (1997).
[36] J. H. Rose, J. P. Vary, and J. R. Smith, Phys. Rev. Lett. **53**, 344 (1984); J. H. Rose, J. R. Smith, and J. Ferrante, Phys. Rev. B **28**, 1835 (1983).
[37] J. Tateno, Solid State Commun. **10**, 61 (1972).
[38] K. K. Nanda, Eur. J. Phys. **19**, 471 (1998).
[39] C. Kittel, *Introduction to Solid State Physics*, 5th ed. (Wiley, New York, 1976).
[40] W. A. Harrison, *Electronic Structure and the Properties of Solids* (Freeman, San Francisco, 1980).
[41] W. A. Harrison (private communication).
[42] B. Pluis *et al.*, Surf. Sci. **239**, 282 (1990); *CRC Handbook of Chemistry and Physics* (CRC Press, Boca Raton, FL, 1977).
[43] D. J. Wales and R. S. Berry, J. Chem. Phys. **92**, 4473 (1990).
[44] M. Schmidt, R. Kusche, B. v. Issendorf, and H. Haberland, Nature (London) **393**, 238 (1998).
[45] H. Röder, E. Hahn, H. Brune, J. P. Bucher, and K. Kern, Nature (London) **366**, 141 (1993).
[46] M. G. Mitch *et al.*, Phys. Rev. Lett. **67**, 875 (1991).
[47] P. M. Ajayan and S. Iijima, Nature (London) **361**, 333 (1993).